Article

Noninvasive and Reversible Cell Adhesion and Detachment via Single-Wavelength Near-Infrared Laser Mediated Photo-isomerization

Wei Li, Zhaowei Chen, Li Zhou, Zhenhua Li, Jinsong Ren, and Xiaogang Qu

J. Am. Chem. Soc., **Just Accepted Manuscript** • DOI: 10.1021/jacs.5b03872 • Publication Date (Web): 28 May 2015

Noninvasive and Reversible Cell Adhesion and Detachment via Single-Wavelength Near-Infrared Laser Mediated Photo-isomerization

Wei Li,[†‡] Zhaowei Chen,[†‡] Li Zhou,[†‡] Zhenhua Li,[†‡] Jinsong Ren*[†] and Xiaogang Qu*[†]

[†] State Key Laboratory of Rare Earth Resources Utilization and Laboratory of Chemical Biology, Changchun Institute of AppliedChemistry, Chinese Academy of Sciences, Changchun 130022, China

[‡]Graduate School of the Chinese Academy of Sciences, Beijing 100039, China

KEYWORDS. Upconversion, spiropyran, cell, photoswitch, interaction.

ABSTRACT: Dynamically regulating cell-molecule interactions is fundamental to a variety of biological and biomedical applications. Herein, for the first time, by utilizing spiropyran conjugated multi-shell upconversion nanoparticles (UCNPs) as a new generation of single-wavelength NIR-controlled photoswitch, we report a simple yet versatile strategy for controlling cell adhesion/detachment reversibly and noninvasively. Specifically, the two-way isomerization of the photoswitch was merely dependent on the excitation power density of the 980 nm laser. At high power density, the ring-opening was prominent, whereas its reverse ring-closing process occurred upon irradiation by the same laser but with the lower power density. Such transformations made the interactions between spiropyran and cell surface protein fibronectin switchable, thus leading to reversible cell adhesion and detachment. Moreover,efficient adhesion-and-detachment of cells could be realized even after 10 cycles. Most importantly, the utilization of NIR not only showed little damage towards cells, but also improved penetration depth. Our work showed promising potential for in vivo dynamically manipulating cell-molecule interactions and biological process.

Introduction

Dynamically regulating the interactions between specific molecules and cell-surface molecules is critical for cell biology due to its potential to attain unprecedented levels of control over diverse cell behaviors even cell fate.[1] Specially, reversible control strategies, which enable real-time alternating such interactions between on-off states, have attracted particular attention since they can aid in the development of high-contrast optical bioimaging[2] and advanced therapies such as cell-based diagnostics[3] and immunotherapy.[4] For instance, reversible manipulation of polymeric materials and immune-cells interactions has been proposed to promote anti-tumor immunity.[4a]Although promising, the further cilnical application of these reversible methods was limited by the invasive and destructive implantable procedures.Thus, it still remains a big challenge to find an appropriate approach to regulate cell-molecule interactions facilely, reversibly and noninvasively.

Among the various control strategies,[5]photomodulation has proven to be an ideal option, by which cell-molecule interactions can be readily controlled with noninvasive property and high spatiotemporal precision.[5a-d] Particularly, photoswitching systems that undergo photo-isomerization reactions have been used to reversibly guide cell-molecular recognition in interfacial systems.[6]Despite its usefulness, the photoswitches typically need to be modified with biomolecules, which requires complicated synthesis and even causes a distortion of the compounds.[7]An intriguing exception is the photochromic spiropyran. Unlike common photochromic systems, spiropyran itself with two different polar isomerizations have shown to be able to reversibly intercalate into DNA helix,[8] regulate enzyme activity[9] and even specifically interact with cell surface protein fibronectin.[10] However, the need for two wavelength light - toxic ultraviolet and low penetrating visible light for ring-opening (350 nm) and ring-closing (560 nm) interconversion processes and the difficulties in focusing the two light beams precisely would complicate the practical process. Moreover, the inevitable cellular damage and poor tissue-penetration of the light used would limit their further biomedical applications. Recently, lanthanide-doped upconversion nanoparticles (UCNPs) have attracted much attention in nanobiotechnology due to their unique photophysical properties.[11]Generally, they can emit UV, visible, and/or near-infrared (NIR) light upon NIR excitation with a large anti-Stokes shift, which has been used to biologically friendly tune photo-isomerization processas reported byour group[12] and others.[13]Specially, Branda and co-workers reported that the emission of an individual core-shell-shell UCNP can be modulated between UV and visible light by changing just the power intensity of one single 980 nm excitation

SCHEME 1. Schematic illustration of the utilization of spiropyran conjugated multi-shell upconversion nanoparticle (SP-UCNP) as a NIR-triggered photoswitch for noninvasive and reversible control of cell adhesion/detachment by merely altering the power density of a single-wavelength 980 nm laser. At high power (8 W/cm2) density, the UCNPs can emit UV photons and activate the isomerization from the spiro (SP) form to the merocyanine (MC) form, resulting in the detachment of cell. Conversely, when exposed to low power (0.5 W/cm2) density, the same UCNPs can emit visible light to drive the MC form back to the SP form, leading to cell adhesion again.

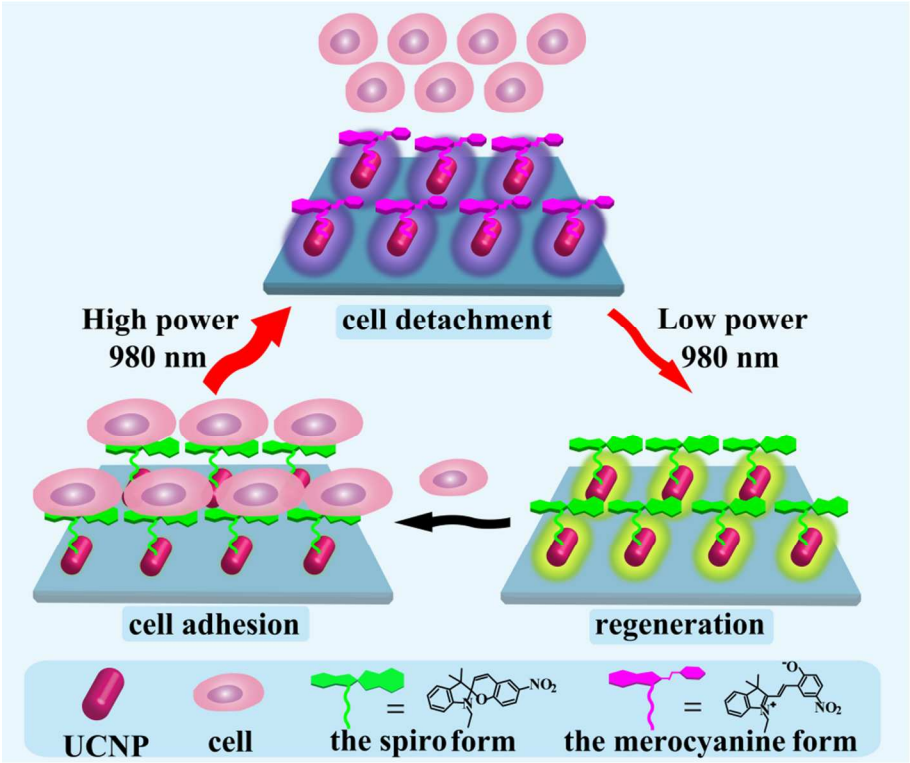

light, which offered a simple wayto regulate photochemical reactions.[14] Accordingly, by taking advantage of this unique feature, we envision thatmodulating thephotochromic of spiropyran with this single-wavelength excited UCNP would provide a convenient but novel way to reversibly control the interactions between spiropyran and cells, which however has remained unexplored until now.

Herein, for the first time, by utilizing spiropyran conjugated multi-shell UCNP (SP-UCNP) as a new generation of single-wavelength NIR-controlled photoswitch, we report a simple yet versatile strategy for controlling cell adhesion/detachment reversibly and noninvasively. In this system, the isomerization of spiropyrans was merely dependent on the excitation power density of the 980 nm NIR laser(Scheme S1). As illustrated in Scheme 1, at high power density, the UV emissions from UCNPs were prominent and that, in turn, induced the formation of ring-opening merocyanine (MC) isomers. This isomerization process could be reversed by just reducing the power density to the point where the visible emission dominated. Such transformations made the interactions between spiropyran and cell surface protein fibronectin switchable, thus leading to reversible cell adhesion and detachment. Moreover, owing to the reversibility and the excellent photostability of the photoswitch, efficient adhesion-and-detachment of cells could be realized even after 10 cycles. Most importantly, the utilization of NIR not only showed little damage towards cells, but also improved penetration depth. We foresee that this new concept may hold great potential for biomedical application, especially for in vivo tissue engineering and medical implantation *et al*.

Results and Discussion

To minimize the energy loss induced by surface quenching effect,[15] we deposited a protecting layer of inert $NaYF_4$ onto the core-shell-shell UCNP[14,16](layer-by-layer seed-mediated shell growth process and the enhanced luminescence intensity, for more details see the Supporting Information, Figure S1, S2 respectively). Transmission electron microscopy (TEM,Figure 1a) demonstrated the as-designed core-shell-shell-shell UCNPs with an average size of 40×60nm (width × length). The typical *d*-spacing value of 0.52 nm (high-resolution TEM, Figure 1b) and X-ray diffraction analysis (Figure S3) illustrated their single hexagonal-phase crystals. Subsequently, a 10-nm-thick (Figure 1c) silica shell was coated on the UCNPs by microemulsion method (UCNP@SiO_2),[12a] which enabled efficient energy transfer between spiropyran and UCNPs. Furthermore, energy dispersive spectroscopic (EDC) element mapping of Si, Y, Yb, Tm and Er also verified the composition of the nanoparticles. After functionalized with (3-aminopropyl)-triethoxysilane (APTES), the resulting nanohybrids (UCNP@SiO_2-NH_2) were further covalently conjugated with carboxyl-containing spiropyran (SP-COOH, Scheme S2 and Figure S4).The surface modification processes (Scheme S3) were confirmedby Fourier transform infrared (FTIR, Figure S5) spectrum and the typical aryl nitro stretching (1338,

1523 cm^{-1}) and acylamide vibration (1650 cm^{-1}) indicated the successful preparation of SP-UCNPs.

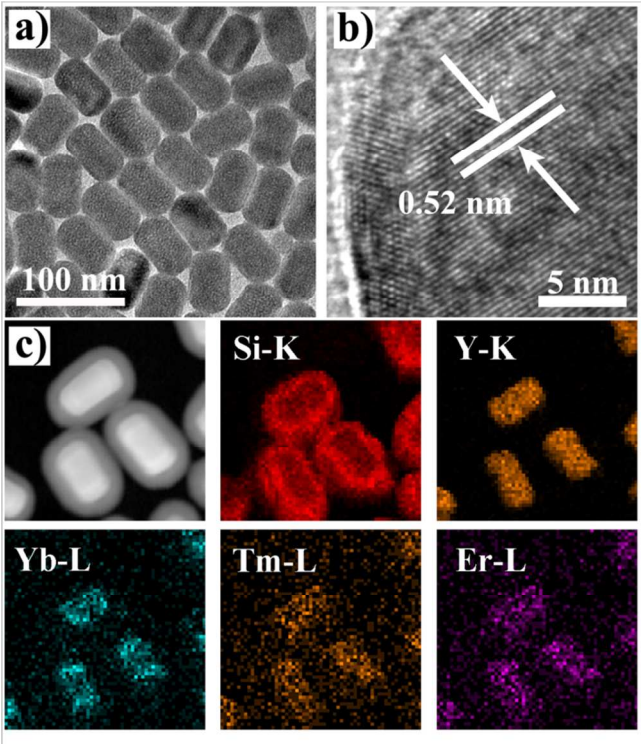

Figure 1. Structural characterization of the as-synthesized multi-shell UCNPs. a) TEM image of $NaYF_4$:Tm/Yb@ $NaYF_4$@ $NaYF_4$:Er/Yb@ $NaYF_4$ core-shell-shell-shell UCNPs. b) High-resolution TEM image of a single UCNP. c) Dark-field TEM image of UCNP@SiO_2 and corresponding energy dispersive spectroscopic (EDC) element mapping of Si K-edge, Y K-edge, Yb L-edge, Tm L-edge and Er L-edge signals.

Next, we investigated the optical properties of SP-UCNP at high (8 W/cm^2) and low (0.5 W/cm^2) power densities of 980 nm NIR laser excitations. The maximum absorption peaks of the ring-closed spiro (SP) form located at 350 nm which overlaps well with the UV emission of the UCNPs (attributed to $^1I_6 \rightarrow {}^3F_4$ (347nm) and $^1D_2 \rightarrow {}^3H_6$ (365nm) transitions of Tm^{3+} ions) under high power density excitation (Figure 2a). This indicated that high power NIR excited UCNPs could be utilized to induce the ring-opening reaction of SP to MC through energy transfer process. The energy transfer process was verified by the significant quenching of upconversion fluorescence (UCL) emission around 350 nm, and the energy transfer efficiency was measured to be 75.76%. As illustrated in Figure S6, exposure of SP-UCNPs solution to high power density excitation resulted in an observable change in color from yellow to violet and a new band around 560 nm. The absorption strength increased over time and reached equilibrium within 6 min. Notably, merely reducing the excitation power density to 0.5 W/cm^2 would facilitate the overlap of the characteristic absorption of MC form at 560 nm and the visible emissions of the UCNPs generated from $^2H_{11/2} \rightarrow {}^4I_{15/2}$ (520 nm) and $^4S_{3/2} \rightarrow {}^4I_{15/2}$ (540 nm) transitions of Er^{3+} ions (Figure 2b), which could in turn be applied to trigger the reverse photoreactions. The energy transfer efficiency was calculated to be 68.8%, which certified the successful interconversion process. Additionally, the solution turned back to yellow and the band at 560 nm disappeared upon exposing to low power 980 nm irradiation for 10 min, (Figure S7), revealing the complete photo-isomerization from MC to SP. The excitation-density-dependent UCL emission was attributed to the nonlinearity of the upconversion mechanisms, where higher excitation power density was needed to achieve a UV-emission-dominated spectral profile by first saturating other visible transitions.[17]These results clearly showed that the reversible two-way photoswitching of spiropyran could be driven by a single-wavelength NIR, and the direction of the photo-isomerization could be modulated by merely increasing (for ring-opening) and decreasing (for ring-closing) the power density. The reversibility of the SP-UCNP photoswitch was tested by monitoring the absorbance at 560 nm while continuously alternating the power density between high/low (10 cycles). As shown in Figure 2c and Figure S8, the photo-isomerization with high/low NIR was reversible and the efficiency of the switching was unaffected, confirming the robustness of SP-UCNP conjugation, which was mainly due to the attenuation of photofatigue by the utilization of noninvasive NIR.[18] Taking together, these results indicated that a new generation of photoswitch system was successfully built, which would facilitate the reversible control of cell adhesion/detachment.

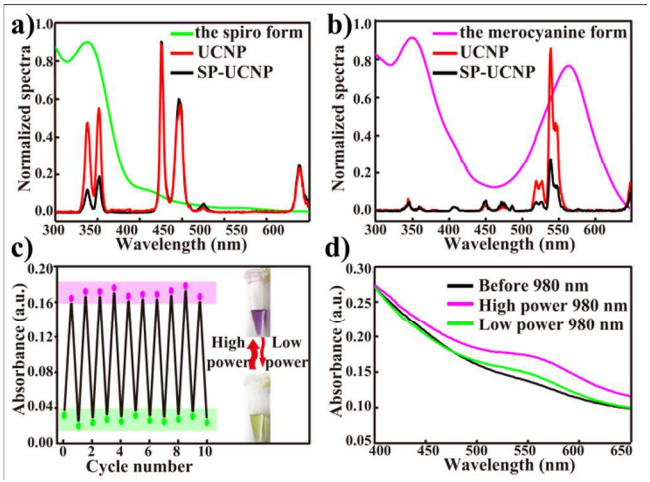

Figure 2. Optical characterization of the as-synthesized SP-UCNPs. a) UV-Vis absorption spectra of the SP form in DMF solvent and the upconversion luminescence (UCL) emission spectrum of UCNPs and SP-UCNPs under high power density (8 W/cm^2) of 980 nm NIR laser. b) UV-Vis absorption spectra of the MC form in DMF solvent, and the UCL emission spectrum of UCNPs and SP-UCNPs at lower power density (0.5 W/cm^2) of 980 nm NIR laser. c) Irradiation cycles of SP-UCNPs; Inset in (c):photographs ofSP-UCNPs in DMF solvent under high power NIR and low power NIR respectively. d) UV-Vis absorption spectra of SP-UCNPs modified surface before and subsequentlyirradiated with high /low power NIR laser.

In the following, we tested the photoswitching ability of SP-UCNP for regulating cell adhesion/detachment. Firstly, we succeeded in fabricating the SP-UCNP modified surface by attaching UCNP@SiO_2-NH_2 to the amino group functionalized glass surface through glutaraldehyde and conjugatingSP-COOH to the UCNPs with the grafting amount calculated to be 7.1 wt % (Scheme S4 and Figure S9). The SEM image revealed the uniform topography of the UCNP@SiO_2-NH_2 deco-

rated surface (Figure S10) and the X-ray Photoelectron Spectroscopy (Figure S11, S12) confirmed the successful procedure. As illustrated in UV/Vis absorption spectra (Figure 2d), when exposure to 980 nm laser at high power density, the SP-UCNP modified surface exhibited an obvious enhancement band around 560 nm, certifying the ring-opening process. In contrast, the characteristic band disappeared after exposure to low power density of NIR, which ensuring the effective ring-closing of spiropyran. The distinct change confirmed that the SP-UCNP on surface could be also effectively triggered by just modulating the power density of NIR laser, thus allowing the single-wavelength NIR mediated interfacial dynamic processes.

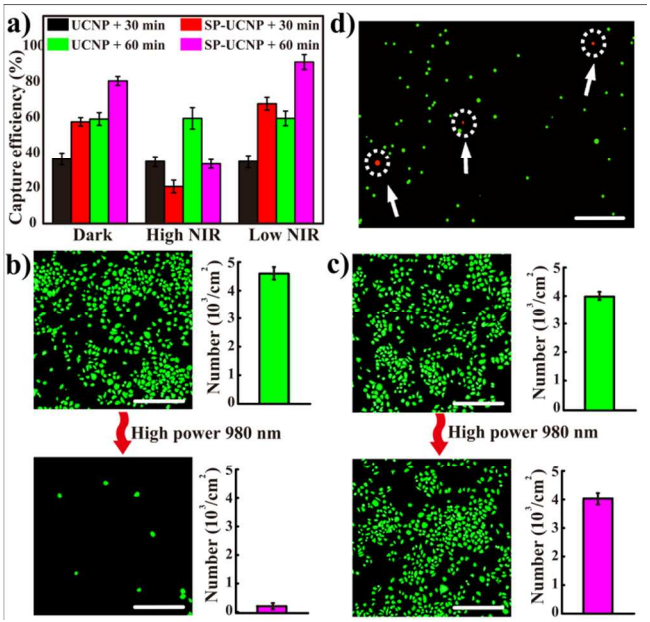

Figure 3. Single-wavelength 980 nm NIR regulates cell adhesion/detachment using the SP-UCNPs. a) After treatment with different illuminations, cell capture efficiency of UCNPs modified surface and SP-UCNPs modified surface at varied time intervals. Fluorescence images of high power (8 W/cm^2) NIR induced cell detachment on b) the system we designed and the system c) without spiropyran. Scale bars are 100 μm. d) Viability of released cell assessed with a live (green)/dead (red) assay.

Afterwards, we performed cell adhesion/detachment experiment via a single wavelength NIR. Before cell adhesion, the modified surfaces were treated with different illuminations. Then HeLa cell suspensions (10^6cells ml^{-1}) in a DMEM medium were incubated with the surfaces and the amount of adhered cells was counted by a hemacytometer at varied time intervals (Figure 3a). Initially, the spiropyran were mainly in the SP form and the SP-UCNP modified surface demonstrated higher capture efficiency compared with the UCNP@SiO_2-NH_2 modified surface, which could be attributed to the specific interaction between SP isomerization and cell surface fibronectin protein.[10]Irradiation at high power density of 980 nm laser gave rise to the MC form and a decrease in capture efficiency was observed, owing to the weak interaction between the MC form and fibronectin.[12a,19,20]Moreover, the low-power NIR illustrated surface displayed the highest capture efficiency among all the surfaces, further confirming that the SP-UCNP could be used as a new generation of photoswitch to guide cell adhesion. We then examined whether the utilization of a single-wavelength NIR could dynamically alter cell adhesion. After a 4h's incubation, the surfacewas gently washed with PBS, stained with calcein (AM) dyes, imagined and counted under a microscopy. As showed in Figure 3b, over 95% original adherent cells were released from the SP-UCNPs based platform after exposure to high power 980 nm for 15 minutes (2.5 min break after 2.5 min irradiation to avoid heating effect of 980 nm laser). In contrast, no obvious detachment from the parallel surface(Figure 3c) was observed. These results confirmed that high power density of 980 nm laser could be applied to induce the photo-isomerization in SP-UCNP photoswitch and further triggered the change of cell adherent behavior of the surface.Moreover, Live/Dead staining method (Figure 3d) were used to verify the good viability of cells released from the surface, which was necessary for practical cell culture and single cell analysis. In addition, the released cells remained functional and spread normallyafter recultured on the glass slide (Figure S13), confirming that the SP-UCNP-basedsystemcould be used as an effective non-invasive cell adhesion/detachment platform for further biological investigations.

Another apparent advantage of the SP-UCNP-based system is the ease of reversibly regulating cell adhesion/detachment on demand. By merely reducing the power density to 0.5 W/cm^2 and kept irradiating for 20 min, the surface could be reused for multiple cycles study. As demonstrated in Figure 4a, b and S14, even after 10 cycles, the platform still showed high efficiency to cell detachment, which could be attributed to the outstanding reversibility and photostability of our NIR-triggered SP-UCNP photoswitch. Furthermore, the spatial control of cell adhesion was also demonstrated by alternating the power density between "high" and "low" site (Figure 4c), which provided an alternative method for cell patterning. Additionally, we investigated the feasibility of this system for application in deep tissues by using pork tissues as a model (Figure 4d, Scheme S5). As expected, only a slightly reduced efficiency was observed for the NIR-triggered platform. In stark contrast, the cell release efficiency with UV irradiation decreased dramatically when came to the tissue study, although direct exposure to UV showed a much high efficiency than NIR. Importantly, the SP-UCNP decorated surface showed good reversibility even in tissue study (Figure S15). Taken together,these results verified that the utilization of NIR controlled SP-UCNP as a new generation of photoswitch not only greatly enhanced the reversibility of the platform and enabled spatial control of cell adhesion/detachment, but also significantly improved penetration depth.

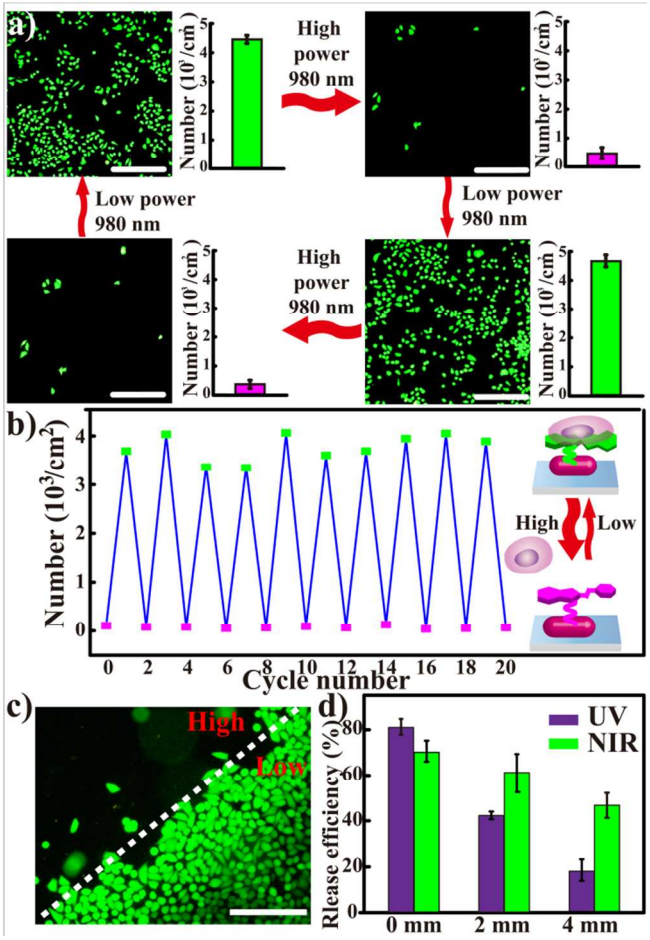

Figure 4. Single-wavelength 980nm NIR regulates reversible control of cell adhesion and detachment. a), b) Reversible adhesion and detachment of cells on SP-UCNPs modified system. Scale bars are 100 μm. c) NIR-induced detachment of cells with pattern light irradiation. Scale bars are 100 μm. d) Cell release efficiency induced by UV and NIR through 0, 2 or 4 mm of pork tissue.

Conclusion

In summary, for the first time, noninvasive and reversible regulation of cell-molecules interaction was successfully realized by utilizing spiropyran conjugated multi-shell UCNP as a single-wavelength NIR-controlled photoswitch. Notably, cell adhesion/detachment can be switched conveniently by merely decreasing/increasing the excitation power density of the same 980 nm laser, which greatly simplified the treatment process. Moreover, efficient adhesion-and-detachment of cells was achieved even after 10 cycles based on the reversiblephotoisomerization reactionsand the excellent photostabilityof the photoswitch. Most importantly, the utilization of NIR not only showed little damage towards cells, but also significantly improved penetration depth, which is superior for further application. We anticipate that this single-wavelength NIR controlled approach would be further developed for in vivo dynamic control of biological process, tissue engineering and medical implantation.

Experimental Section

Materials. All reagents and solvents were commercially available and used as received without further purification.

Synthesis of β-$NaYF_4$:Tm/Yb core nanoparticles. Briefly, 1.4 mmol of YCl_3•$6H_2O$, 0.6 mmol $YbCl_3$•$6H_2O$ and 0.01 mmol of $TmCl_3$•$6H_2O$ were added to a 100 ml flask containing12 ml oleic acid and 30 ml octadeceneand heated to 160℃ to form a homogeneous solution.The temperature was then lowered to 50℃ and the flask was placed under nitrogen gas protection. Once the reaction reached 50℃, 10 ml methanol solution containing NH_4F (296 mg, 8.0 mmol) and NaOH (200 mg, 5.0 mmol) were added in and kept stirring for 30 min. Afterslowly evaporated the methanol and heated the mixture to 300℃ for 1.5 h under nitrogen protection, the solution was cooled downed and the resulting nanoparticleswere purified by addition of ethanol, collected by centrifugation and finally re-suspended in 10 ml cyclohexane.

Synthesis of $NaYF_4$:Tm/Yb@$NaYF_4$ core-shell nanoparticles. 1.8 mmol of YCl_3•$6H_2O$ was added to a 100 ml flask containing12 ml oleic acid and 30 ml octadeceneand heated to 120℃. The temperature was lowered to 80℃ and the dispersion of $NaYF_4$:Tm/Yb core nanoparticles in hexanes were added. Afterslowly evaporated the hexanes and heated to 110℃, the mixture was cooled down to 50℃. Once the temperature reached 50℃, 10 ml methanol solution containing NH_4F (259 mg, 7.0 mmol) and NaOH (175 mg, 4.4 mmol) was added in and kept stirring for 30 min. Afterslowly evaporated the methanol and heated the mixture to 300℃ for 1.5 h under nitrogen protection, the solution was cooled downed and the resulting nanoparticleswere purified by addition of ethanol, collected by centrifugation and finally re-suspended in 10 ml cyclohexane.

Synthesis of $NaYF_4$:Tm/Yb@$NaYF_4$@$NaYF_4$:Er/Ybcore-shell-shell nanoparticles. The same procedure outlined above for the synthesis of core-shell $NaYF_4$: Tm/Yb@$NaYF_4$ was employed except that the core-shell nanoparticle was used as core and YCl_3•$6H_2O$ was used as precursor for epitaxial shell growth.

Synthesis of $NaYF_4$:Tm/Yb@$NaYF_4$@$NaYF_4$:Er/Yb@$NaYF_4$core-shell-shell-shell nanoparticles. The same procedure outlined above for the synthesis of core-shell $NaYF_4$: Tm/Yb@$NaYF_4$ was employed except that the core-shell-shell nanoparticle was used as core and YCl_3•$6H_2O$ was used as precursor for epitaxial shell growth.

Synthesis of SP-COOH. During the synthesis, all the reaction vessels were wrapped in aluminum foil to ensure the reaction was performed in the dark.The preparation of the carboxy-containing spiropyran 1'-(β-carboxyethyl)-3', 3'-dimethyl-6-nitrospiro [indoline-2', 2-chromane] was performed as our reported paper.[12]In brief, 0.06 mol of 2, 3, 3-trimethylindole-nine, 0.06 mol of 3-iodopropanoic acid and 5 ml of ethyl methyl ketone were refluxed under nitrogen at 100℃ for 3 h. The resulting mixture was dissolved in water, and the solution was washed with chloroform.After theevaporation of water, 1-(β-carboxyethyl)-2, 3, 3-tri-methylindolenine iodide was achieved. Next, 0.04 mol of the resulting iodide, 0.04 mol of 5-nitrosali-cylaldehyde and 3.8 ml (0.04 mol) piperidine were dissolved in ethyl methyl ketoneand refluxed for 3 h. On standing overnight, a yellow crystalline powder was precipitated. The product was filtered and washed with methanol to

yield SP-COOH (70% yield).The product was characterized by ^{1}HNMR spectroscopy as shown in Figure S1.^{1}HNMR (400 MHz, $CDCl_3$, 25℃, TMS): δ = 1.0-1.3 (6H; 2CH_3), 2.6 (2H; CH_2COO), 3.4-3.5 (2H; CH_2N), 5.9-6.0 (2H; olefinic protons), 6.6-8.2 (aromatic protons).

Preparation of silica coated UCNP. Firstly, 7.2 ml triton, 28 ml cyclohexane, 7.2 ml hexanol, 680μl water and 50 mg of UCNPs were mixed in a 100 ml flask by sonication and agitation for 40 min.Then,100 μl of TEOS was added drop wise into the mixture. Afterward, 160μl NH_3•H_2O was added into the flask and stirred for 24 h. The resulting nanoparticles were precipitated out by the addition of ethanol to yield UCNPs@SiO_2.

Preparation of amino functionalized UCNP@SiO_2. Briefly, 20 mg of UCNPs@SiO_2 and 30 ml toluene were firstly mixed in a 100 ml flask and heated to 110℃. Next, 30μl of (3-1minopropyl) trierhoxysilane (APTES) was added drop wise into the mixture. After stirring for 24 h, the precipitates were separated by centrifugation, washed with ethanol three times, and dried at 60℃ for 12 h to obtain the UCNPs@SiO_2-NH_2.

Preparation of spiropyran conjugated UCNP@SiO_2-NH_2. During the synthesis, all the reaction vessels were wrapped in aluminum foil to ensure the reaction was performed in the dark. 0.526 mmol of SP-COOH (200 mg) was firstly dissolved in 30 ml dimethylformamide (DMF). 4 ml MES buffer (pH 6.0, 20 mM) containing EDC (500 mg) and NHS (400 mg) was added into the solution and agitated for 1.5 h. Afterwards, 100 mg UCNPs@SiO_2-NH_2in 4 ml MES buffer was added in and stirred for 48 h. The resulting nanoparticles were washed by water and DMF.

Preparation of the UCNPs Modified Substrate. The glass slide of 1×1cm were cleaned and immersed into 10 ml 0.5% APTES solution for 1 h to introduce amino group. Then the amine terminated substrates were reacted with the solution of UCNPs@SiO_2-NH_2 (10 ml/ml) for 24 h at room temperature.

Preparation of the SP-UCNPs Modified Surface. Firstly, SP-COOH (200mg, 0.526mmol) was dissolved in 30 ml DMF. Then EDC (500 mg) and NHS (400 mg) in 4mml MES buffer (pH 6.0, 20 nM) was added to the solution. After agitating the solution overnight in the dark, the UCNPs modified surfaces were immersed into the solution for 24 h to conjugate with SP-COOH through EDC/NHS chemistry. The grafting amount of spiropyran on the UCNPs was calculated by UV/Vis spectra.

NIR triggeredPhoto-isomerization of the SP-UCNPs on modified surface. Before exposure to NIR illumination, the absorption spectra of the SP-UCNPs modified surfaces were recorded on JASCO V-550 UV-Vis spectrophotometer.Subsequently, the surface was immersed in 500ul of DMF and exposed to high power NIR irradiation for 5 min. The surfaces were dried out quickly before being measured. Afterwards, the surface was immersed in 500ul of DMF, exposed to low NIR irradiation for another 15 min and measured again.

Cell Culture. The Hela cells were cultured at 37℃ in an atmosphere of 5% (v/v) CO_2 in Dulbecco's modified Eagle's medium (DMEM) supplemented with 10% fetal bovine serum(FBS). The media was changed every three days, and the cells were digested by trypsin and re-suspended in fresh complete medium before plating.

Cell Adhesion. The UCNP modified surface and SP-UCNP modified surface were pre-treated with different illumination. Afterwards, they were placed into a size-matched 24-well Lab-TekTM Chamber Slide. Hela cells were added to each culture flask to obtain a cell density of 1×10^6 cells per flask. The flasks were cultured in DMEM containing 10% FBS at 37℃ in an atmosphere of 5% CO_2. After incubating for 30 min and 1 h, the surfacewas gently washed with PBS for 3 times, and cell numbers in supernatant was counted by a hemacytometer again. The number of adhesion cells ($n_{adhesion}$) on the surfaces and the capture efficiency (e) can be calculated by the following equations respectively:

$$n_{adhesion} = n_{total} - n_{supernatant}$$

$$e = n_{adhesion} / n_{total}$$

NIR controlled Cell Detachment. After incubated with cells for 4 h, the platform was examined for NIR triggered release. Irradiation NIR laser at the powers density of 8 W/cm^2 for 15min (2.5 min break after 2.5 min irradiation to avoid heating effect of 980 nm laser), the surface was gently washing with PBS in 15 s to remove the release cells. Fluorescent microscopic imaging was used to monitor the cell release. For live/dead cell staining, the released cell was collected from the washing buffer by centrifugation at 1000 rpm for 5 min, and then propidium iodide (PI) and calcein (AM) dyes were added into the released cell. After 15 min incubation, the cells were imaged by the microscope. For repeatability study, the substrates firstly were digested by trypsin and washed with PBS for 3 times. Then the substrates were exposed to NIR at the powers of 0.5 W/cm^2 for 20 min and reused for cell adhesion and detachment.Furthermore, to control cell detachment regionally, we firstly treated the SP-UCNP modified surfaces with a dose of 20 min lower power NIR illuminations and then incubated them with cells. Afterwards, we shield the surfaces with a light-proof photomask on one half and put the surfaces under high power density NIR for 15 min. As the light source and photomask were removed, the surfaces were washed gently with PBS and recorded with microscope. For deep tissue irradiation, pork tissues (muscle tissue) with 0 mm, 2 mm, 4 mm thickness was placed above the cell adhesive surface with a distance of 1 mm. The laser was irradiation from the top of tissue.

Fluorescent Microscopic Imaging. For the imaging test, the surfacewas placed into a 24-well plates and incubated with a density of 1×10^6 cell/well for 4 h at 37℃ in an atmosphere of 5% CO_2. AM dyes were added into the flask for 15 min. Then the substrates were gently washed with PBS and finally imaged under an Olympus BX-51 optical equipped with a CCD camera. After NIR irradiation, the substrates were gently washed with PBS, stained with AM for 15 min and viewed under the microscope.

ASSOCIATED CONTENT

Supporting Information.Detailed experimental procedures and supplementary figures and tables.This material is available free of charge via the Internet at http://pubs.acs.org.

AUTHOR INFORMATION

Corresponding Author

jren@ciac.ac.cn; xqu@ciac.ac.cn

ACKNOWLEDGMENT

We thank Wen Li from Graduate School of the Chinese Academy of Sciences for the helpful advice on the manuscript. Financial support was provided National BasicResearch Program of China (Grant 2012CB720602,2011CB936004) and the National Natural Science Foundationof China (Grants 91213302, 21210002, 21431007, 91413111).

REFERENCES

(1)(a) Hynes, R. O. *Science***2009**, 326, 1216; (b)Herbert, S. P.; Stainier, D. Y. R. *Nat. Rev. Mol. Cell Biol.***2011**, 12, 551; (c) Robertus, J.; Browne, W. R.; Feringa, B. L. *Chem. Soc. Rev.***2010**, 39, 354;(d) Stevens, M. M.; George, J. H. *Science***2005**, 310, 1135.

(2)(a) Kim, Y.; Jung, H.-y.; Choe, Y. H.; Lee, C.; Ko, S.-K.; Koun, S.; Choi, Y.; Chung, B. H.; Park, B. C.; Huh, T.-L.; Shin, I.; Kim, E. *Angew. Chem. Int. Ed.* **2012**,*51*, 2878;(b) Takahashi, S.; Piao, W.; Matsumura, Y.; Komatsu, T.; Ueno, T.; Terai, T.; Kamachi, T.; Kohno, M.; Nagano, T.; Hanaoka, K. *J. Am. Chem. Soc.* **2012**,*134*, 19588.

(3)Liu, Q.; Wu, C.; Cai, H.; Hu, N.; Zhou, J.; Wang, P. *Chem. Rev.* **2014**,*114*, 6423.

(4)(a) Ali, O. A.; Huebsch, N.; Cao, L.; Dranoff, G.; Mooney, D. J. *Nat. Mater.***2009**,*8*, 151;(b) Kim, J.; Li, W. A.; Choi, Y.; Lewin, S. A.; Verbeke, C. S.; Dranoff, G.; Mooney, D. J. *Nat.Biotechnol.***2015**,*33*, 64;(c) Okano, F.; Merad, M.; Furumoto, K.; Engleman, E. G. *J.Immunol.***2005**,*174*, 2645.

(5)(a) Lee, T. T.; García, J. R.; Paez, J. I.; Singh, A.; Phelps, E. A.; Weis, S.; Shafiq, Z.; Shekaran, A.; del Campo, A.; García, A. J. *Nat. Mater.***2015**,*14*, 352;(b) Li, W.; Wang, J.; Ren, J.; Qu, X. *Angew. Chem. Int. Ed.* **2013**,*52*, 6726;(c) Li, W.; Wang, J.; Ren, J.; Qu, X. *J. Am. Chem. Soc.* **2014**,*136*, 2248;(d) Liu, D.; Xie, Y.; Shao H.; Jiang X. *Angew. Chem. Int. Ed.* **2009**,*48*, 4406;(e) Hou, S.; Zhao, H.; Zhao, L.; Shen, Q.; Wei, K. S.; Suh, D. Y.; Nakao, A.; Garcia, M. A.; Song, M.; Lee, T.; Xiong, B.; Luo, S.-C.; Tseng, H.-R.; Yu, H.-h. *Adv. Mater.* **2013**,*25*, 1547;(f) Liu, H.; Li, Y.; Sun, K.; Fan, J.; Zhang, P.; Meng, J.; Wang, S.; Jiang, L. *J. Am. Chem. Soc.* **2013**,*135*, 7603;(g) Zhang, P.; Chen, L.; Xu, T.; Liu, H.; Liu, X.; Meng, J.; Yang, G.; Jiang, L.; Wang, S. *Adv. Mater.* **2013**,*25*, 3566;(h) Zhang, Z.; Chen, N.; Li, S.; Battig, M. R.; Wang, Y. *J. Am. Chem. Soc.* **2012**,*134*, 15716.

(6)Weber, T.; Chandrasekaran, V.; Stamer, I.; Thygesen, M. B.;Terfort, A.; Lindhorst, T. K. *Angew.Chem. Int. Ed.* **2014**,*53*, 14583.

(7) (a) Schönberger, M.; Trauner, D. *Angew. Chem. Int. Ed.* **2014**,*53*, 3264;(b) Zhang, J.; Zou, Q.; Tian, H. *Adv. Mater.***2013**,*25*, 378.

(8) Andersson, J.; Li, S.; Lincoln, P.; Andréasson, J. *J. Am. Chem. Soc.* **2008**,*130*, 11836.

(9) Song, Y.; Xu, C.; Wei, W.; Ren, J.; Qu, X. *Chem.Commun.* **2011**,*47*, 9083.

(10)(a) Higuchi, A.; Hamamura, A.; Shindo, Y.; Kitamura, H.; Yoon, B. O.; Mori, T.; Uyama, T.; Umezawa, A. *Biomacromolecules***2004**,*5*, 1770;(b) Wang, N.; Li, Y.; Zhang, Y.; Liao, Y.; Liu, W. *Langmuir* **2014**,*30*, 11823;(c) Edahiro, J.-i.; Sumaru, K.; Tada, Y.; Ohi, K.; Takagi, T.; Kameda, M.; Shinbo, T.; Kanamori, T.; Yoshimi, Y. *Biomacromolecules***2005**,*6*, 970.

(11)(a) Cheng, L.; Yang, K.; Li, Y.; Chen, J.; Wang, C.; Shao, M.; Lee, S.-T.; Liu, Z. *Angew. Chem. Int. Ed.* **2011**,*50*, 7385;(b) Huang, P.; Zheng, W.; Zhou, S.; Tu, D.; Chen, Z.; Zhu, H.; Li, R.; Ma, E.; Huang, M.; Chen, X. *Angew. Chem. Int. Ed.* **2014**,*53*, 1252;(c) Liu, J.; Liu, Y.; Liu, Q.; Li, C.; Sun, L.; Li, F. *J. Am. Chem. Soc.* **2011**,*133*, 15276;(d) Liu, Y.; Chen, M.; Cao, T.; Sun, Y.; Li, C.; Liu, Q.; Yang, T.; Yao, L.; Feng, W.; Li, F. *J. Am. Chem. Soc.* **2013**,*135*, 9869;(e) Yang, Y.; Shao, Q.; Deng, R.; Wang, C.; Teng, X.; Cheng, K.; Cheng, Z.; Huang, L.; Liu, Z.; Liu, X.; Xing, B. *Angew. Chem. Int. Ed.* **2012**,*51*, 3125; (f) Liu, J.; Liu, Y.; Bu, W.; Sun, Y.; Sun, Y.; Du, J.; Shi, J. *J. Am. Chem. Soc.* **2014**,*136*, 9701.

(12)(a) Chen, Z.; Zhou, L.; Bing, W.; Zhang, Z.; Li, Z.; Ren, J.; Qu, X. *J. Am. Chem. Soc.* **2014**,*136*, 7498;(b) Zhou, L.; Chen, Z.; Dong, K.; Yin, M.; Ren, J.; Qu, X. *Adv. Mater.* **2014**,*26*, 2424.

(13)(a) Lai, J.; Zhang, Y.; Pasquale, N.; Lee, K.-B. *Angew.Chem. Int. Ed.* **2014**,*53*, 14419;(b) Min, Y.; Li, J.; Liu, F.; Yeow, E. K. L.; Xing, B. *Angew. Chem. Int. Ed.* **2014**,*53*, 1012;(c) Wang, L.; Dong, H.; Li, Y.; Xue, C.; Sun, L.-D.; Yan, C.-H.; Li, Q. *J. Am. Chem. Soc.* **2014**,*136*, 4480;(d) Zhang, B. F.; Frigoli, M.; Angiuli, F.; Vetrone, F.; Capobianco, J. A. *Chem.Commun.***2012**,*48*, 7244;(e) Zhang, C.; Xu, C.-H.; Sun, L.-D.; Yan, C.-H.*Chem. Asian J.***2012**,*7*, 2225; (f) Liu, J.; Bu, W.; Shi, J. *Angew. Chem. Int. Ed.* **2013**,*52*, 4375; (g) Yang, T.; Liu, Q.; Li, J.; Pu, S.; Yang, P.; Li, F., *RSC Adv.***2014**,*4*, 15613; (h) Boyer, J.-C.; Carling, C.-J.; Chua, S. Y.; Wilson, D.; Johnsen, B.; Baillie, D.; Branda, N. R., *Chem. Eur. J.***2012**,*18*, 3122.

(14)Boyer, J.-C.; Carling, C.-J.; Gates, B. D.; Branda, N. R. *J. Am. Chem. Soc.* **2010**,*132*, 15766.

(15)(a) Han, S.; Deng, R.; Xie, X.; Liu, X. *Angew. Chem. Int. Ed.* **2014**,*53*, 11702;(b) Peng, J.; Xu, W.; Teoh, C. L.; Han, S.; Kim, B.; Samanta, A.; Er, J. C.; Wang, L.; Yuan, L.; Liu, X.; Chang, Y.-T. *J. Am. Chem. Soc.* **2015**,*137*, 2336.

(16)(a) Wang, F.; Deng, R.; Wang, J.; Wang, Q.; Han, Y.; Zhu, H.; Chen, X.; Liu, X. *Nat. Mater.***2011**,*10*, 968;(b) Wen, H.; Zhu, H.; Chen, X.; Hung, T. F.; Wang, B.; Zhu, G.; Yu, S. F.; Wang, F. *Angew. Chem. Int. Ed.* **2013**,*52*, 13419.

(17)(a) Pollnau, M.; Gamelin, D. R.; Lüthi, S. R.; Güdel, H. U.; Hehlen, M. P. *Phys. Rev. B* **2000**,*61*, 3337;(b) Shen, J.; Chen, G.; Ohulchanskyy, T. Y.; Kesseli, S. J.; Buchholz, S.; Li, Z.; Prasad, P. N.; Han, G. *Small* **2013**,*9*, 3213.

(18)Tong, R.; Hemmati, H. D.; Langer, R.; Kohane, D. S. *J. Am. Chem. Soc.* **2012**,*134*, 8848.

(19)Gelmi, A.; Zanoni, M.; Higgins, M. J.; Gambhir, S.; Officer, D. L.; Diamond, D.; Wallace, G. G. *J. Mater.Chem. B* **2013**,*1*, 2162.

(20)Bergkvist, M.; Carlsson, J.; Oscarsson, S. *J. Biomed.Mater. Res. Part A***2003**,*64A*, 349.

Graphic Table of Content